Limestone assimilation and the origin of CO2 emissions at the Alban Hills (Central Italy): constraints from experimental petrology.

Giada Iacono-Marziano, Fabrice Gaillard, Michel Pichavant

Limestone assimilation and the origin of CO_2 emissions at the Alban Hills (Central Italy): constraints from experimental petrology

Giada Iacono Marziano[a*], Fabrice Gaillard[b], Michel Pichavant[b]

[a] Istituto Nazionale di Geofisica e Vulcanologia sezione di Palermo, Palermo, Italy;

[b] Institut des Sciences de la Terre d'Orleans, UMR 6113 CNRS, Orléans, France

* Corresponding author; g.iacono@pa.ingv.it

Abstract

The Alban Hills volcanic region (20 km south of Rome, in the Roman Province) emitted a large volume of potassic magmas (> 280 km^3) during the Quaternary. Chemical interactions between ascending magmas and the ~7000-8000-m-thick sedimentary carbonate basement are documented by abundant high temperature skarn xenoliths in the eruptive products and have been frequently corroborated by geochemical surveys. In this paper we characterize the effect of carbonate assimilation on phase relationships at 200 MPa and 1150-1050°C by experimental petrology. Calcite and dolomite addition promotes the crystallization of Ca-rich pyroxene and Mg-rich olivine respectively, and addition of both carbonates results in the desilication of the melt. Furthermore, carbonate assimilation liberates a large quantity of CO_2-rich fluid. A comparison of experimental versus natural mineral, glass and bulk rock compositions suggests large variations in the degree of carbonate assimilation for the different Alban Hills eruptions. A maximum of 15 wt% assimilation is suggested by some melt inclusion and clinopyroxene compositions; however, most of the natural data indicate assimilation of between 3 and 12 wt% carbonate. Current high CO_2 emissions in this area most likely indicate that such an assimilation process still occurs at depth. We calculate that a magma intruding into the carbonate basement with a rate of ~1-2•10^6 m^3/year, estimated by geophysical studies, and assimilating 3-12wt% of host rocks would release an amount of CO_2 matching the current yearly emissions at the Alban Hills. Our results strongly suggest that present CO_2 emissions in this region are the shallow manifestation of hot mafic magma intrusion in the carbonate-hosted reservoir at 5-6 km depth, with important consequences for the present-day volcanic hazard evaluation in this densely populated and historical area.

Introduction

Central-Southern Italy is a complex geodynamic province characterized by large-scale extensional tectonism associated with the eastward migration of the Apennine Chain and the opening of the Tyrrhenian Sea (Turco and Zuppetta, 1998 and references therein; Barberi et al., 1994; Peccerillo, 2005 and references therein). The extension-related Quaternary volcanism consists of numerous active, dormant, and extinct volcanoes that produced a relatively important volume of alkaline rocks (Peccerillo, 2005). Among them, the Roman Magmatic Province was active from 800 to 20 ka and probably represents the largest known center of potassic magmatism (Peccerillo, 2005). The erupted products, dominantly composed of pyroclastic deposits, amount to a volume of 900 km^3 over an area of ~6400 km^2 (Giordano et al., 2006; Peccerillo, 2005). Four volcanic centers, from north to south Mts. Vulsini, Mt. Vico, Mts. Sabatini and Alban Hills, are all characterized by large multiple calderas and are emplaced on a thick Mesozoic-Cenozoic carbonate sedimentary pile, identified at depths between 1 and ca. 7-8 km (Barberi et al., 1994; Parotto and Praturlon, 2004; Gaeta et al., 2006). All magmas emitted in the Roman Magmatic Province are potassium rich (K_2O/Na_2O between 1 and 10), consistently with a metasomatized phlogopite-rich mantle source (Conticelli, 1998; Peccerillo, 1999; Elkins-Tanton and Grove, 2003; Peccerillo, 2005). Large variations in the degree of silica-saturation of the volcanic products are also acknowledged (Nappi et al., 1995; Kamenetsky et al., 1995; Trigila et al., 1995; Perini et al., 2000; Peccerillo, 2005; Gaeta et al., 2006): the erupted compositions range between quartz normative (trachy-basalt to trachyte) and strongly silica-undersaturated (tephrite / foidite to phonolite), with the most silica-undersaturated magmas belonging to the Alban Hills volcanic center. Figure 1 shows the bulk rock compositions of Alban Hills, Vulsini and Vico eruptive products in a Total Alkali versus Silica (TAS) diagram. Although large variations are evident in both silica and alkali contents for the three volcanic centers, the silica poorest compositions were clearly erupted at the Alban Hills.

At the Alban Hills, the magmatic reservoir that fed the largest past eruptive events (e.g. Trigoria-Tor de Cenci and Villa Senni eruptions) was interpreted to be located in or at the base (~3-6 km depth) of the carbonate sequence (Freda et al., 1997; Palladino et al., 2001; Giordano et al., 2006). Despite the absence of volcanic activity younger than 19 ka (Voltaggio and Barbieri, 1995), the Alban Hills system is considered as quiescent on the basis of geophysical studies that indicate a low-velocity region more than 5 km beneath the youngest craters, shallower frequent seismic activity and significant volcano uplift (Amato and

Chiarabba, 1995; Chiarabba et al., 1997; Feuillet et al., 2004; Marra et al., 2004). Moreover, the region is currently characterized by important CO_2 emissions of deep origin (Chiodini and Frondini, 2001; Carapezza et al., 2003; Gambardella et al., 2004), as is most of Central-Southern Italy (Gambardella et al., 2004; Chiodini et al., 2004). This CO_2 is directly discharged from several gas vents (23-25°C, Hooker et al., 1985; Minissale, 2004) and dissolved in shallow ground waters, sometimes reaching strong CO_2 over-saturation and generating sudden gaseous emissions with elevated gas hazard, such as in 1995 (Chiodini and Frondini, 2001). In all, CO_2 discharged by the Alban Hills region was estimated > $4.2*10^9$ mol/year over an area of 1500 km^2 (Chiodini and Frondini, 2001; Gambardella et al., 2004). Zones with high CO_2 fluxes are generally centered above structural highs and faults within the sedimentary basement (Chiodini and Frondini, 2001). CO_2 origin is still debated in the absence of recent volcanic activity: deep magma degassing, metamorphic decarbonation of limestone and mantle degassing and have been proposed (Chiodini and Frondini, 2001; Gambardella et al., 2004; Chiodini et al., 2004). He and C isotopic compositions of the gases emitted by several gas vents suggest a magmatic contribution for He and a dominant CO_2 contribution from the decarbonation of sedimentary limestone (Hooker et al., 1985; Giggenbach et al., 1988; Chiodini and Frondini, 2001). The $\delta^{13}C$ of the emitted CO_2 ranges from -3.5 to +0.9 ‰ vs. PDB, strongly deviating from mantle signatures ($\delta^{13}C$: 4-7 ‰, Deines, 2002; Hekinian et al 2000 and references therein). The most positive $\delta^{13}C$ values of the emitted CO_2 are associated to the highest $^3He/^4He$ ratios of the volcanic district: R/Ra=1.54 (Chiodini and Frondini, 2001 and references therein).

Important interactions between the carbonate host rocks and the magmas are documented by abundant, high temperature, calcic skarn xenoliths found in the volcanic products (Federico et al., 1994; Trigila et al., 1995; Peccerillo, 2005) and by the coexistence of magmatic (leucite and clinopyroxene) and skarn (garnet, vesuvianite, wollastonite, spinel) minerals within the wall rock/magma chamber interface (Federico and Peccerillo, 2002; Dallai et al., 2004). The oxygen isotopic composition of magmatic minerals has been shown to record such large scale interaction. Indeed, the high $\delta^{18}O$ measured in leucite, sanidine and, to a lesser extent, in clinopyroxene most likely reveals magma contamination by sedimentary carbonate in the upper crust (Turi and Taylor, 1976; Dallai et al., 2004; Peccerillo, 2005). The degree of assimilation remains, however, difficult to evaluate because a major part of the oxygen deriving from the carbonate escapes as CO_2 during the assimilation. Moreover, most workers concluded that any crustal assimilation (and limestone assimilation above all) would

essentially lead to a dilution of trace elements in the magma, since Roman mafic magmas are considerably more enriched in incompatible elements than the local crustal rocks (Peccerillo 2005 and references therein). A quantitative assessment of carbonate assimilation is therefore difficult using classical geochemical tracers (Conticelli, 1998; Peccerillo, 2005). First order attempts to quantify the degree of assimilation were approximated by mass balance calculations on major elements during crystal fractionation + assimilation and suggested that an assimilation of 3 to 5 wt% calcite to would be consistent with the liquid line of descent at the Alban Hills (Gaeta et al., 2006).

With this paper, we intend to quantify the degree of carbonate assimilation that occurred at depth in the Alban Hills plumbing system and to assess the contribution of this process to the current important CO_2 emissions in this area. At first, an experimental study is presented to quantify the importance of the carbonate assimilation process at the Alban Hills, using phase relationships and liquid line of descent as an indicator of the degree of assimilation. Then, we estimate the quantity of CO_2 liberated by carbonate assimilation in the plumbing system of the Alban Hills and compare it to the measured current CO_2 fluxes (Chiodini and Frondini, 2001; Gambardella et al., 2004). We finally propose a prospective view of the Alban Hills plumbing system integrating geophysical, geochemical and petrological constraints with important implications for the present-day volcanic hazard evaluation in this densely populated and historical area.

2. Experimental Methods

In contrast to previous experimental studies on the petrology of the Alban Hills magmas (Trigila et al., 1995; Freda et al., 1997), which investigated the effect of gaseous CO_2 on phase relationships, our experiments were performed on mixtures of a mafic end-member with carbonates and therefore also illustrate the effect of CaO and MgO addition to the magma.

A mafic lava, AH7a, has been used as starting composition. This rock was collected in a lava flow of the Alban Hills (Mt. Mellone) and has been dated at 308 ka (Gaeta et al., 2006). According to Gaeta et al. (2006) it represents the most primitive magmatic liquid found at Alban Hills, on the basis of its high MgO content and low Na_2O content. Rock powders of AH7a were first melted in air at 1350°C for 3 hours. Then the recovered glass was hydrated in an internally heated pressure vessel (IHPV) at 200 MPa, 1250°C, for 5 hours. One wt% of water was initially loaded in the capsule but the recovered glass contained more water (Table

1) due to hydrogen incorporation during the hydrothermal treatment (Gaillard et al., 2003). Starting from this primitive hydrous melt, we investigated the consequence of different degrees of carbonate assimilation on phase relationships. The hydrous glass was therefore mixed with variable amounts of Ca carbonate (Carrara Marble) and Ca, Mg carbonate (dolomite); the amount of added carbonates ranged between 0 and 18 wt% of the experimental charge. For selected experiments, an additional amount of water (1.5wt%) was introduced within the experimental assemblage. Arc-welded $Au_{80}Pd_{20}$ capsules were used to avoid Fe loss. The experiments lasted 24 hours and were performed in internally heated pressure vessels at 200 MPa, consistently with the estimated depth of crustal magma storage beneath the Alban Hills (Chiarabba et al., 1997; Freda et al., 1997; Feuillet et al., 2004; Giordano et al., 2006). The experimental temperatures were 1150, 1125, 1100 and 1075°C, nearly covering the entire course of magma crystallization from near-liquidus to near-solidus. In order to maintain highly oxidizing conditions during the experiments, the autoclave was pressurized with pure Argon. A Ni-Pd redox sensor placed in experiment #1100 measured redox conditions around 2 log units above the nickel-nickel oxide buffer. After rapid drop quench, the samples were polished and examined by optical microscope and scanning electron microscope. Phase compositions of the experimental samples were analyzed by an SX 50 electron microprobe. Conditions used were 15 kV, 6 nA, 10 sec on peak and 5 sec on background. Selected samples were analyzed by Karl Fisher titration to determine their water content (Table 1) and then used as internal standards, together with the dry starting glass, to evaluate the water contents of the other samples from the total of the microprobe analysis (Devine et al., 1995, analytical error ~ 0.6 wt% H_2O).

Mass balance calculations were performed to compute phase proportions (glass, minerals and fluid phase) in the experimental charges, taking into account the compositions of the starting mixtures (including H_2O and CO_2), the residual melt (included dissolved H_2O) and the mineral phases (Table 1 and 2). The amount of dissolved CO_2 in carbonate-added glasses was arbitrarily fixed at 0.2 wt%, based on accepted solubility models (Newman and Lowernstern, 2002; Papale et al, 2006), considering that variations up to 0.6 wt% in the CO_2 content of the glasses have been tested to have a negligible effect on the mass balance calculations. Indeed, the most important source of error in our calculation is the water content in the glass, which propagated through the mass balance equations, gives us an averaged uncertainty of ±1 wt% on the fluid phase proportion and of ±5 wt% on the fluid phase composition. Therefore, to improve the estimation of H_2O amounts dissolved in the glass and fluid phase abundances, we

introduced in the mass balance calculations a relationship between H_2O wt% in the glass and X_{H_2O} in the gas based on the solubility model of Newman & Lowernstern (2002).

3. Results: phase relationships and evolution of the residual liquid

Phase proportions and glass composition of each experimental sample are listed in Table 1, together with the experimental conditions and the composition of the starting glass. In carbonate-free conditions, all the samples are water-undersaturated and no fluid phase is observed. The liquidus temperature for the investigated composition with 1.7 wt% water is ~ 1150°C, in view of the very low crystal content observed in the samples 1150/1 and in agreement with the results of Trigila et al. (1995) for a similar composition at comparable experimental conditions. At 1100 and 1075°C, we estimated by mass balance an average crystal content of ~36 and 60 wt%, respectively. The clinopyroxene (cpx) is present over the entire crystallization range, however, substantial variations in its composition are observed from 1150 to 1075°C (Table 2). High temperature cpx is Si-Mg-rich and Al-Fe-poor. With decreasing temperature, cpx becomes Al-richer and Si-poorer. Leucite and phlogopite appear at lower temperatures: 1100 and 1075°C, respectively.

In carbonate-bearing charges, we did not observe any immiscible carbonate-rich phase. All the calcium and magnesium were incorporated in the magma (silicate) and CO_2 was dominantly incorporated into the fluid component. Carbonate addition considerably increases the crystallization of the melt and the stability fields of cpx and leucite. The latter appears at 1150°C for 10wt% CaCO3 added (#1150/5). Globally, the CaO content of cpx increases from 22 to 25wt% as Ca-carbonate is added up to ~15 wt%. We also noted a strong increase in the ferric iron content in cpx (calculated after Lindsley, 1983) with addition of carbonate. As for carbonate free-conditions, high temperature cpx is Si-Mg-rich and becomes Al-Fe-richer as fractionation proceeds. Olivine is only observed in experimental charges doped in dolomite (1150/3; 1125/2; 1100/4; 1075/5). These olivine crystals are Mg- and Ca-rich (Table 2). Phlogopite crystallization is also generally promoted by dolomite addition. The addition of extra water (1.5 wt%) reduces the degree of crystallization and, in particular, the leucite stability field (see #1100/5;1075/6;1125/3). A fluid phase appears in the form of abundant bubbles with a few weight percent of carbonate addition, and reaches values > 9 wt% when ~18 wt% of carbonate is added.

The silica content of the residual liquid decreases with carbonate addition as illustrated in the TAS diagram in Fig.2a. In this projection, the effects of Ca and Mg-carbonate on the residual

liquid composition are very similar. This figure shows that the AH7a composition (SiO_2~48wt%; Na_2O+K_2O~9wt%) with no carbonate addition evolves toward liquids with higher silica and alkali contents (at 1075°C: SiO_2 ~ 52wt% and Na_2O+K_2O ~ 14wt%), whereas the same starting composition assimilating carbonate evolves toward residual liquids substantially poorer in silica with similar alkali contents (at 1075°C and 15 wt% calcite: SiO_2 ~ 41wt% and Na_2O+K_2O ~ 14wt%). Carbonate addition triggers the mafic composition AH7a to fractionate toward strongly silica undersaturated foiditic compositions whereas a carbonate-free parental magma would generate phonolitic residual liquid.

The CaO contents of the residual liquids in near-liquidus experiments (#1150) strongly increase with calcite addition. In contrast, at lower temperature most of the calcium liberated by the dissolution of calcite is incorporated into the Ca-rich cpx. The CaO content of the residual liquid exceeds 15wt% only in the experimental charges with more than 10wt% of calcite addition. Figure 3a illustrates this relative CaO enrichment in the liquid. This diagram shows that the effect of cpx crystallization upon cooling is to decrease both the MgO content and the CaO/Al_2O_3 ratio of the residual liquid. With addition of Ca-carbonate, the CaO/Al_2O_3 ratio shows less decrease during crystallization, remaining almost constant when 14-18 wt% of carbonate is added. Compared to Figure 2a, this projection shows how calcite and dolomite addition have contrasting effects on the residual liquid composition, in which the residual liquids of dolomite-doped charges (grey dots) are richer in MgO and much less enriched in CaO than the liquids of calcite-doped experiments (black dots).

4. Discussion

4.1. Mechanisms of carbonate assimilation

The added carbonates are completely consumed by reactions that modify the melt compositions, produce a CO_2-rich fluid phase, and result in precipitation of cpx, and olivine (in dolomite-doped experiments). Calcite is dominantly assimilated following the general reaction:

$$CaCO_3 + 2\ SiO_2 + MgO \Rightarrow CaMgSi_2O_6 + CO_2 \quad (1)$$

While the magnesite end-member reacts with the silicate via:

$$2\ MgCO_3 + SiO_2 \Rightarrow Mg_2SiO_4 + 2CO_2 \quad (2)$$

Reaction (1) is deduced from the calcium-rich cpx analyzed in calcite doped charges and reaction (2) is supported by Mg-rich olivine only observed in dolomite doped experiments (See Table 2). Assimilation of dolomite involves both reactions (1) and (2) to produce cpx

and olivine. In both mechanisms (1) and (2), carbonate assimilation results in the diminution of magmatic SiO_2 as we observed in our experimental charges (Table 1; Figure 2). The desilication of the residual liquid is therefore the most important geochemical consequence of carbonate assimilation.

4.2. Carbonate vs. CO_2 effect

In the literature on Alban Hills magmatic processes, high CO_2 fugacity or high CO_2/H_2O ratio during magma formation and differentiation are often mentioned as responsible for the observed liquid line of descent (Freda et al., 1997; Palladino et al., 2001; Peccerillo, 2005). The CO_2 effect, however, substantially differs from the effect of carbonate assimilation that we describe above. Hereafter, we briefly clarify this crucial distinction.

Trigila et al. (1995) and Freda et al. (1997) presented experimental data on the effect of CO_2 on phase equilibrium relationships for an Alban Hills mafic composition relatively similar to ours. In both cases, the experiments were performed at pressures of 1 atm, 200 and 400 MPa, with temperatures ranging between 1015 and 1230°C and fluid phase compositions varying from pure water to pure CO_2. CO_2 was added as Ag_2CO_3, in contrast to our study where Ca—Mg carbonate were added. Their experimental results of CO_2-rich experiments show that the crystallization of cpx and leucite controls the liquid line of descent, similar to our findings. However, except for a few runs in Trigila et al (1995), their experiments showed that crystallization of the magma induces an enrichment in silica and alkalis similarly to our experiments in which no carbonate was added (Fig. 2a). The main effect of carbonate assimilation shown by our experiments is an important decrease in the silica content of the residual liquid, coupled with an increase in the alkali content during crystallization due to both reaction (1) and (2) (Fig.2a). Furthermore, the desilication of the residual liquid (reaction (1) and (2)) occurs for very low carbonate additions (<3 wt%). Hereafter we identify evidence of carbonate contamination in the magmatic product of the Alban Hills, essentially on the basis of the degree of silica-depletion during magmatic differentiation.

4.3. Quantitative assessment of limestone assimilation

Cpx and leucite, often accompanied by oxides, were the main crystallizing phases in the experimental charges, while plagioclase was never observed, in agreement with the reported mineralogical assemblages of Alban Hills lavas (Trigila et al., 1995). Figure 2 compares in a TAS projection the compositions of the experimental residual liquid to the bulk rocks and

glass inclusions from the Alban Hills available in the literature, compiled according to their age (see figure caption). Figures 2b and 2c distinguish eruptive products from the post-caldera (<350 ka, according to De Rita et al., 1988; Giordano et al., 2006) and the pre-caldera (>350 ka) periods, respectively. Crystallization of the AH7a composition in the absence of added carbonate reproduces a very minor portion of the observed compositional variation among natural samples. In contrast, AH7a crystallization with variable degrees of carbonate assimilation (up to 14-18 wt%) produces residual liquids covering the whole compositional range of Alban Hills eruptive products erupted before and after the major collapse of the caldera. Most of the natural compositions are consistent with assimilation of 3 and 12 wt% carbonate, however a few compositions fall into the fields consistent with no assimilation and with 14-18 wt % assimilation (Fig. 2b, 2c). In Figure 3, the same compositions as in Figure 2 are plotted in a CaO/Al_2O_3 vs. MgO diagram, which illustrates the chemical evolution of the residual liquids during crystallization and highlights Ca and Mg-enrichment due to carbonate assimilation. High temperature liquids plot in the MgO-rich part of the diagram. Upon cooling, cpx crystallization forces the liquid to evolve toward Al-rich and Mg-Ca-poor compositions. Calcite addition limits the decrease of the CaO/Al_2O_3 ratio in the residual liquid with cpx crystallization. Dolomite addition has a much slighter effect on the CaO/Al_2O_3 ratio, while substantially increasing the MgO content of the residual liquids. As in Figure 2, the Alban Hills compositional range reported in Figures 3b and 3c cannot be solely explained by crystal fractionation from the AH7a composition. The range of CaO/Al_2O_3 ratio displayed by natural composition reveals that the magmas have undergone an extremely variable amount of carbonate assimilation, up to > 9 wt% of Ca-carbonate. The comparison between Figures 2 and 3 gives important information about the assimilation process. Bulk-rock and melt compositions consistent with the highest degree of assimilation in the TAS plots are also consistent with the highest degree of assimilation in the CaO/Al_2O_3 vs. MgO diagrams. However, the assimilation degrees observed in Figure 2 are generally higher than in Figure 3, indicating important contributions from dolomite assimilation (probably up to half of the total input), which has an important effect on the desilication of the residual liquid, but a negligible one on its CaO/Al_2O_3 ratio. The highest degrees of assimilation are associated with two melt inclusion compositions entrapped in cpx phenocrysts with SiO_2 ~42wt%, Na_2O+K_2O ~11wt% and CaO/Al_2O_3 ratios of ~0.8, similarly to the liquid that we obtained by adding 14.5wt% of calcite to AH7a (Tab.1, sample 1125/1). It is interesting to note that the extent of assimilation suggested by Figures 2 and 3 did not substantially change between the pre- and post-caldera periods. In both cases, extremely variable amounts of assimilation can be deduced from

different eruptive events and, sometimes, within a single event. For example, the Villa Senni eruptive event (labeled VSEU~360 ka), a major phase of the Alban Hills activity, consists of lower and upper flow units separated by lithic breccias (Freda et al., 1997). The time interval between the two flows is not precisely known (Giordano et al., 2006). The upper flow unit is more primitive (Mg-richer) and its fractionation trend indicates a negligible degree of carbonate assimilation and follows our residual liquid compositions obtained when less than 3% carbonate is added (Fig. 2b and 3b). Freda et al. (1997) obtained a similar differentiation trend in their experiments with CO_2-H_2O mixtures. In contrast, the lower flow unit that shows a more fractionated composition apparently assimilated up to 7wt% $CaCO_3$. Both bulk rock (closed circles) and melt inclusion (open circles) compositions are consistent with this interpretation (Fig. 2b and 3b). This heterogeneity in the degree of assimilation is probably a feature of carbonate-magma interactions, as suggested by field studies. Barnes et al. (2005) studied a 466 Ma (Barnes et al., 2006) years old magmatic intrusion in carbonate and silicate rocks, outcropping in Norway, where massive carbonate assimilation is revealed by the crystallization of Ca-rich pyroxene and by the desilication of the magma, similarly to reaction (1). Such an assimilation process is described over a several kilometers wide zone, which shows extreme heterogeneities in terms of bulk rock compositions, but similar mineral compositions and assemblages (Barnes et al., 2003, 2005). Indeed, dioritic (weak assimilation), syenitic and monzonitic (important assimilation) rocks coexist in the form of sheets within the magmatic complex. Mutual intrusive relationships are also commonplace as evidence of magma mingling. Magma emplacement most probably consisted of repeated injection of hundreds of subhorizontal sheet-like bodies (Barnes et al., 2003; Barnes et al., 2006) that experienced different degrees of assimilation. We propose that limestone assimilation occurred similarly in the plumbing system of the Alban Hills, producing compositionally inhomogeneous and not well mixed magmas in the reservoir prior to the eruption.

Selected compositions of cpx and olivine are shown in Table 2 and compared to natural cpx and olivine from the Alban Hills. The experimental cpx varies greatly from high Mg, Si contents and low Fe, Al contents at high temperature to low Mg, Si contents and high Al, Fe contents at low temperature. The amount of carbonate added in the charge correlates well with the CaO content of experimental cpx, although CaO variations are restricted between 22 and 25 wt%. In Figure 4, the CaO content of natural and experimental clinopyroxenes is plotted against their Mg# (MgO/(MgO+FeO)). Upon cooling, the experimental cpx tends to become less magnesium-rich and less calcium-rich, for a given amount of carbonate addition. In

natural cpx, the CaO content is variable at high Mg#, but it remains always extremely high with decreasing Mg#, suggesting that calcite assimilation up to 15 wt% mainly occurs at high temperature (1100-1150°C). Only for few natural cpx the silica and alkali contents of the hosting rock are available (Aurisicchio et al., 1988) and suggest a good agreement between whole rock and cpx compositions in terms of assimilation degree. Cpx compositions compatible with 0wt% carbonate assimilation crystallized in silica-rich (>47 wt%), alkali-poor (Na_2O+K_2O < 9wt%) rocks, also compatible with no carbonate assimilation. In contrast, cpx compositions compatible with significant carbonate assimilation (~10 wt%) crystallized in silica-poor (<43 wt%), alkali-rich (Na_2O+K_2O > 9wt%) rocks, also compatible with high degrees of carbonate assimilation. High temperature experiments doped with dolomite crystallize Mg-rich and Ca-rich olivines similar to those analyzed in ejecta from Alban Hills (Table 2). In these ejecta, Federico et al. (1994) reported olivine with FeO down to 3.7 wt%, CaO up to 1wt% and very low NiO contents that do not indicate a mantle origin. Federico et al. (1994) proposed that such olivine could derive from high temperature reaction between the magma and the calcareous-dolomitic sequences below Alban Hills, as effectively confirmed by our experimental data.

The chemical variability displayed by natural products in Fig. 2 and 3 cannot be reproduced solely by the crystallization of the mineralogical assemblages observed in Alban Hills lavas (mainly Cpx and leucite). Indeed such a closed system crystallization cannot account for the important desilication of the melt (from 48-50 wt% down to 42-44 wt%) concurrent with CaO and alkali increase. Only an addition of Ca-Mg carbonate to the mafic magma can explain these features. Moreover, cpx and olivine compositions also suggest Mg and Ca-enrichments (Fig. 4) occurring when the high temperature magma (1100-1150°C) comes into contacts with the carbonate rocks. Altogether, it appears that important carbonate-magma exchanges are required to explain compositional and mineralogical variations at the Alban Hills. The frequent occurrence of high temperature skarns (Federico et al., 1994; Trigila et al., 1995; Peccerillo, 2005) and the high $\delta^{18}O$ measured in cpx by Dallai et al. (2004) are further evidence of the carbonate assimilation process. We conclude that the magmatic trends at the Alban Hills can be experimentally reproduced from the AH7a composition assimilating up to 12-15 wt% of carbonate in which the dolomitic component represents an important fraction of the assimilated rocks. However, the possibility that the AH7a lava already results from partial assimilation of carbonate has to be considered. In a parallel study, Iacono Marziano and Gaillard (2006) have shown that a phono-tephritic liquid relatively similar to AH7a can derive from a trachybasalt with SiO_2 ~51 wt% that assimilated ~9wt% of carbonates. Although

magma compositions more primitive and silica-richer than the AH7a one have not been observed at the Alban Hills, trachybasaltic compositions with higher SiO_2 contents have been described at Mts. Vulsini (Kamenetsky et al., 1995, Fig.1). Considering that the Roman Province magmatic products have been proposed to derive from a common mafic source on the basis of isotopes and trace element signatures (Peccerillo 2005 and references therein), the existence of a more primitive composition at the Alban Hills similar to the relatively SiO_2-rich trachybasalt from Mt. Vulsini cannot be excluded. This would imply that the carbonate assimilation process in the Alban Hills plumbing system is more intense than what we estimate with our experiments. Carbonate assimilation degrees could therefore be significantly higher than 15 wt%. Indeed the fields shown in Figures 2, 3, and 4 are specific to the starting composition AH7a. Presumably, carbonate assimilation in some other starting material will result in similar types of fields, but displaced according to the original bulk composition.

The other volcanic centers of the Roman Province emitted generally silica-richer compositions than the Alban Hills (Fig.1) with different mineral assemblages (mainly cpx, olivine and plagioclase phenocrysts in the mafic rocks; Peccerillo, 2005), suggesting lower degrees of interaction with the carbonate rocks. The trachybasaltic magmas from Mt. Vulsini mostly differentiated into trachytes (Fig. 1), as expected from close system fractionation (Iacono Marziano and Gaillard, 2006). However, Figure 1 also shows the existence at Mts. Vulsini of phonolitic compositions and tephritic-foiditic compositions comparable to the ones of the Alban Hills in terms of silica and alkali contents. This probably implies that variable carbonate assimilation by trachybasaltic primitive magmas also occurred at Mts. Vulsini.

4.4. Origin of CO_2 emissions and volcanic hazard at the Alban Hills

Considering a maximum CO_2 solubility in the melt of 0.5 wt% at 200 MPa from solubility data relevant to our compositions (Thibault and Holloway, 1994), 10wt% of carbonate assimilation would imply that ~ 5 wt% of the Alban Hills magma consisted of CO_2-rich fluid phase. However, as discussed above, the degree of carbonate assimilation at this volcanic center was probably inhomogeneous in space and time giving a variable production of CO_2 up to ~7 wt% (corresponding to 15 wt% of assimilated $CaCO_3$). Such high fluid contents in the magma reservoir undoubtedly affected both the magma ascent and the eruptive dynamics (Huppert and Woods, 2002). Indeed, high CO_2 content has been proposed to be at the origin

of the highly energetic eruptions at the Alban Hills (Palladino et al., 2001). An important question to evaluate is to what extent the CO_2 produced by assimilation coexists with, or rapidly separates from the magma, subsequently generating important degassing events.

Presently, the Alban Hills region is characterized by large CO_2 emissions. This CO_2 is dominantly dissolved into shallow groundwaters and sometimes directly released into the atmosphere by localized gas vents. Chiodini and Frondini (2001) estimated a continuous CO_2 injection into the aquifers exceeding $4.2 \bullet 10^9$ mol/year and a gas flow rate of $0.6 \bullet 10^9$ mol/year from the two largest gas vents. The carbon isotopic signature ($\delta^{13}C$ between -3.5 and +0.9 ‰ vs. PDB) of the gases released by the vents (Chiodini and Frondini, 2001 and references therein) is consistent with an important contribution from marine carbonates ($\delta^{13}C$ of Apenninic carbonates: 2.2 ± 0.66 ‰, Chiodini et al., 2004). Concurrently, the helium isotopic ratio of the emitted gases (R/Ra: 0.94-1.54) is very close to the magmatic values measured in fluid inclusions in olivine and cpx phenocrysts from Alban Hills eruptive products (Martelli et al., 2004) and suggests the presence of a mantle-derived magmatic component (Chiodini and Frondini, 2001 and references therein; Martelli et al., 2004). Gas emissions in the Central-Southern Italy are generally considered to derive from degassing of a mantle source (Chiodini et al., 2000, 2004) metasomatized by the addition of subducted crustal material (Peccerillo, 1999). Nevertheless, the geochemical signature of released gases at the Alban Hills is also compatible with magmatic assimilation and decarbonation of limestone at crustal depth: the released gasses would inherit their helium isotopic signature from the parental magma, while their $\delta^{13}C$ would be controlled by the assimilated limestone. Carbon isotopic fractionation between the melt and the fluid phases remains difficult to quantify in the absence of consistent experimental data in basaltic compositions (Mattey, 1991 and references therein). To quantify the amount of CO_2 produced by magmatic assimilation of limestone and dolostone at the Alban Hills, we assume that: 1) the rate of CO_2 released at depth by assimilation equals the rate of CO_2 emission at surface (steady state transfer); 2) the rate of CO_2 production at depth is directly proportional to the rate of primitive magma currently injected into the carbonate host rocks times the degree of assimilation. Figure 5 shows how increasing degrees of assimilation generate increasing amounts of CO_2 for a given magma intrusion rate into the sedimentary carbonate. Based on the well-documented uplift of the Alban Hills region from 1951 to 1994, Chiarabba et al. (1997) and, more recently, Feuillet et al. (2004) estimated that the corresponding volume of the magma emplaced during this time interval at a depth of ~ 5-6 km would be of ~$40\text{-}94 \bullet 10^6$ m^3 depending on the geometry of the

reservoir considered for their modeling (sill, sphere, dike). This corresponds to a yearly volume of ~1-2•10^6 m^3 of magma injected in the reservoir during the 44-year period. Considering such a rate of primitive magma replenishment within a carbonate hosted reservoir and an assimilation of 3-12 wt% carbonate, as deduced from our experimental data, we calculate an amount of produced CO_2 of 0.8-6.2•10^9 mol/year at depth. This value matches accurately the total CO_2 emissions at surface that have been measured to be 4.8•10^9 mol/year in the Alban Hills area (Chiodini and Frondini, 2001). We therefore suggest here, on the basis of the quantitative agreement between petrology, gas geochemistry and geophysics, that CO_2 emissions at the Alban Hills mainly result from assimilation of sedimentary carbonate during the emplacement of a mafic magma at 5-6 km depth.

It is noteworthy that the magma injection rate for the Alban Hills chamber is comparable to the average intrusion rate estimated for Mt. Vesuvius over the past 25 ka of eruptive activity (~2•10^6 m^3/year, Rosi et al., 1987). This suggests that the Alban Hills plumbing system is still active and that an important volume of magma can be stored in the shallow carbonate reservoir. Moreover, Panza et al. (2007) recently proposed that the mantle source of the Alban Hills magmas could still be productive because S-waves are slowed at depths between 60 and 120 km, suggesting the possible presence of molten material. The conjunction of such evidence requires a careful re-evaluation of the volcanic hazards in this historical and densely populated area.

5. Concluding remarks

An experimental investigation has quantified the amount of sedimentary carbonate assimilated by the Alban Hills magmas in their crustal plumbing system. The study showed that the liquid line of descent from the most primitive mafic composition recognized at Alban Hills requires 0 to 15wt% assimilation in order to explain the compositional range displayed by the eruptive products. Such assimilation explains the large variations in the degree of silica-undersaturation displayed by the magmatic products and corroborates previous geochemical studies revealing important contamination during magma ascent through, and storage within the carbonate crust. Estimated CO_2 production as a consequence of 3-12 wt% of sidewall assimilation has been shown to match present-day emissions of CO_2 in this volcanic area. CO_2 degassing in Central-Southern Italy is a regional process that occurs also in non-volcanic areas. The recycling of sedimentary limestone via the Adriatic subduction and subsequent thermal decomposition of carbonates in the mantle has been proposed as the main

mechanism responsible for the regional CO_2 emissions in Italy. Our work, however, shows that carbonate assimilation in the upper crust can represent an important supplementary mechanism of CO_2 production that quantitatively explains important emissions from active volcanic zones.

Acknowledgements

M. Gaeta is thanked to have provided the sample AH7a. This study was initially supported by the 2005 INGV program: Progetto DPC-INGV-V3 (Colli Albani, responsible P.Scarlato). Funding from the French ANR (Project ELECTROVOLC; contract JC05-42707 allocated to F.Gaillard) allowed this study to be finished. G.Iacono Marziano acknowledges the INGV of Palermo for the postdoctoral grant that permitted her to accomplish this study. Calvin Barnes, Giovanni Chiodini and an anonymous reviewer are thanked for their constructive comments that greatly improved the manuscript.

References:

Amato, A., Chiarabba, C., 1995. Recent uplift of the Alban Hills volcano (Italy); evidence for a magmatic inflation?. Geophys.Res. Lett. 22, 1985-1988.

Aurisicchio, C., Federico, M., Gianfagna, A., 1988. Clinopyroxene chemistry of the High-Potassium Suite from the Alban Hills, Italy. Mineral. Petrol. 39, 1-19.

Barberi, F., Buonasorte, G., Cioni, R., Fiordelisi, A., Foresi, L., Iaccarino, S., Laurenzi, M.A., Sbrana, A., Vernia, L., Villa, I.M., 1994. Plio-Pleistocene geological evolution of the geothermal area of Tuscany and Latium. Memorie Descrittive Carta Geologica d'Italia XLIX, 77–134

Barnes, C.G., Prestvik, T., Barnes, M.A.W., Anthony, E.Y., 2003. Geology of a magma transfer zone: the Hortavær Igneous Complex, north-central Norway, Norsk Geologisk Tidsskrift 83, 187–208.

Barnes, C.G., Prestvik, T., Sundvoll, B., Surratt, D., 2005. Pervasive assimilation of carbonate and silicate rocks in the Hortavær igneous complex, north-central Norway. Lithos 80, 179-199.

Barnes C.G., Li Y., Barnes M., McCullock L., Frost C., Prestvik, T., Allen C., 2006. Carbonate assimilation in the alkaline Hortavær igneous complex. Abstract of the 16th Goldschmidt Conference, Melbourne, Australia.

Carapezza, M. L., Badalamenti, B., Cavarra, L., and Scalzo, A., 2003. Gas hazard assessment in a densely inhabited area of Colli Albani Volcano (Cava dei Selci, Roma). J. Volcanol. Geotherm. Res. 123, 81-94.

Chiarabba, C., Amato, A., and Delaney, P.T., 1997. Crustal structure, evolution and volcanic unrest of the Alban Hills, Central Italy. Bull. Volcanol. 59, 161-170.

Chiodini, G., Frondini, F., Cardellini C., Parello F., Peruzzi, L., 2000. Rate of diffuse carbon dioxide Earth degassing estimated from carbon balance of regional aquifers: the case of central Apennine, Italy. J. Geophys. Res. 105, 8423-8434.

Chiodini, G., Frondini, F., 2001. Carbon dioxide degassing from the Albani Hills volcanic region, Central Italy. Chem. Geol. 177, 67-83.

Chiodini, G., Cardellini, C., Amato, A., Boschi., E., Caliro, S., Frondini F., Ventura, G., 2004. Carbon dioxide Earth degassing and seismogenesis in central and southern Italy. Geophys. Res. Lett. 31, 7, L07615.

Conticelli, S, 1998. The effect of crustal contamination on ultrapotassic magmas with lamproitic affinity: mineralogical, geochemical and isotope data from the Torre Alfina lavas and xenoliths, Central Italy. Chem. Geol. 149, 51-81.

Dallai, L., Freda, C., and Gaeta, M., 2004. Oxygen isotope geochemistry of pyroclastic clinopyroxene monitors carbonate contributions to Roman-type ultrapotassic magmas. Contrib. Mineral. Petrol. 148, 247–263.

Deines, P, 2002, The carbon isotope geochemistry of mantle xenoliths: Earth-Science Reviews, v. 58, p. 247-278.

De Rita, D., Faccenna, C., Funiciello, R., and Rosa, C., 1995. Stratigraphy and volcano-tectonics, in: R. Trigila (Ed.), The Volcano of the Alban Hills, Tipografia S.G.S., Roma, 33-71.

De Rita, D., Funiciello, R., Parotto, M., 1988. Carta Geologica del Complesso Vulcanico dei Colli Albani (scala 1:50.000). Progetto Finalizzato Geodinamica, CNR Roma.

Devine, J.D., Gardner, J.E., Brach, H.P., Layne, G.D., Rutherford, M.J., 1995. Comparison of microanalytical methods for estimation of H2O content of silicic volcanic glasses. Am. Mineral. 80, 319–328.

Elkins-Tanton, L.T., and T.L., Grove, 2003. Evidence for deep melting of hydrous, metasomatized mantle: Pliocene high potassium magmas from the Sierra Nevadas, J. Geophys. Res. 108, 2350, DOI 10.1029/2002JB002168.

Federico, M., Peccerillo, A., Barbieri, M., Wu, T.W., 1994. Mineralogical and geochemical study of granular xenoliths from the Alban Hills volcano, Central Italy: bearing on

evolutionary processes in potassic magma chambers. Contrib. Mineral. Petrol. 115, 384–401.

Federico, M., Peccerillo, A., 2002. Mineral chemistry and petrogenesis of the granular ejecta from the Alban Hills volcano (Central Italy). Mineral. Petrol. 74, 223-252.

Feuillet, N., Nostro, C., Chiarabba, C., and Cocco, M., 2004, Coupling between earthquake swarms and volcanic unrest at the Alban Hills Volcano (central Italy) modeled through elastic stress transfer: J. Geophys. Res. 109, B02308, doi:10.1029/2003JB002419.

Freda, C., Gaeta, M., Palladino, D.M., and Trigila, R., 1997. The Villa Senni (Alban Hills, central Italy): the role of H_2O and CO_2 on the magma chamber evolution and on the eruptive scenario. J. Volcanol. Geotherm. Res. 78, 103–120.

Gaeta, M., Freda, C, Christensen, J.N., Dallai, L., Marra, F., Karner, D.B., and Scarlato, P., 2006. Time-dependent geochemistry of clinopyroxene from the Alban Hills (Central Italy): Clues to the source and evolution of ultrapotassic magmas. Lithos 86, 330-346.

Gaillard, F., Schmidt B.C., Mackwell, S., McCammon, C., 2003. Rate of hydrogen-iron redox exchanges in silicate melts and glasses. Geochim. Cosmochim. Acta 67, 2427-2441.

Gambardella, B., Cardellini, C., Chiodini, G., Frondini, F., Marini, L., Ottonello G., and Vetuschi Zuccolini, M., 2004. Fluxes of deep CO_2 in the volcanic areas of central-southern Italy. J. Volcanol. Geotherm. Res. 136, 31-52.

Giggenbach, W., Minissale, A.A., and Scandiffio, G., 1988. Isotopic and chemical assessment of geothermal potential of Colli Albani area, Latium Region, Italy. Appl. Geochem. 3, 475-486.

Giordano, G., De Benedetti, A.A., Diana, A., Diano, G., Gaudioso, F., Marasco, F., Miceli, M., Mollo, S., Cas, R.A.F., and Funiciello, R., 2006. The Colli Albani mafic caldera (Roma, Italy): Stratigraphy, structure and petrology. J. Volcanol. Geotherm. Res. 155, 49-80.

Hekinian, R., Pineau, F., Shilobreeva, S., Bideau, D., Gracia E., Javoy, M., 2000. Deep sea explosive activity on the Mid-Atlantic Ridge near 34°50′N: Magma composition, vesicularity and volatile content. J. Volcanol. Geotherm. Res. 98, 49-77.

Hooker, P.J., Bertrami, R., Lombardi, S., O'Nions, R.K., Oxburgh, E.R., 1985. Helium-3 anomalies and crust–mantle interaction in Italy. Geochim. Cosmochim. Acta 49, 2505–2513.

Huppert H.E., Woods A.W., 2002. The role of volatiles in magma chamber dynamics. Nature 420, 493-495.

Iacono Marziano, G., Gaillard, F., 2006. Limestone assimilation: an important non magmatic source of volcanic CO_2. Geophysical Research Abstracts, Vol. 8, 08924, 2006.

Kamenetsky, V., Métrich, N. and Cioni, R., 1995. Potassic primary melts of Vulsini (Roman Province): evidence from mineralogy and melt inclusions. Contribution to Mineralogy and Petrology 120, 186-196.

Lindsley, D.H., 1983. Pyroxene thermometry. Am. Mineral. 68, 477-493.

Marra, F., Taddeucci, J., Freda, C., Marzocchi, W., Scarlato, P., 2004. Recurrence of volcanic activity along the Roman Comagmatic Province (Tyrrhenian margin of Italy) and its tectonic significance. Tectonics 43. doi:10.1029/2003TC001600.

Martelli, M., Nuccio, P.M., Stuart F.M., Burgess, R., Ellam, R.M., Italiano, F., 2004. Helium-stronzium isotope constraints on mantle evolution beneath the Roman Comagmatic Province, Italy. Earth Planet. Sci. Lett. 224, 295-308.

Mattey, D.P., 1991. Carbon dioxide solubility and carbon isotope fractionation in basaltic melt. Geochim. Cosmochim. Acta 55, 3467-3473.

Minissale, A., 2004. Origin, transport and discharge of CO_2 in central Italy. Earth Sci. Rew. 66, 89-141.

Nappi, G., Renzulli, A., Santi, P., and Gillot, P.Y., 1995. Geological evolution and geochronology of the Vulsini Volcanic District (central Italy). Boll. Soc. Geol. It. 114, 599–613.

Newman, S., Lowenstern, J.B., 2002. VolatileCalc: a silicate melt–H_2O–CO_2 solution model written in Visual Basic for Excel. Comput. Geosci. 28, 597–604.

Palladino, D.M., Gaeta, M., and Marra, F., 2001. A large k-foiditic hydromagmatic eruption from the early activity of the Alban Hills Volcanic District (Italy). Bull. Volcanol 63, 345–359.

Papale, P., Moretti, R., and Barbato, D., 2006. The compositional dependence of the saturation surface of $H_2O + CO_2$ fluids in silicate melts. Chem. Geol. 229, 78-95.

Panza, G.F., Peccerillo, A., Aoudia, A., Farina, B., 2007. Geophysical and petrological modelling of the structure and composition of the crust and upper mantle in complex geodynamic settings: The Tyrrhenian Sea and surroundings. Earth-Science Reviews 80, 1-46.

Parotto, M., Praturlon, A., 2004. The Souuthern Apennine Arc. In: Crescenti V., D'Offizi S., Merlini S., Sacchi L. (Eds.) Geology of Italy. Spec. Vol., It. Geol. Soc. 32. IGC, Florence, 33-58.

Peccerillo, A., 1998. Relationships between ultrapotassic and carbonate-rich volcanic rocks in central Italy: petrogenetic and geodynamic implications. Lithos 43, 267-279.

Peccerillo, A., 1999. Multiple mantle metasomatism in central-southern Italy: geochemical effects, timing and geodynamic implications. Geology 27, 315–318.

Peccerillo, A., 2005. Plio-Quaternary volcanism in Italy. Petrology, Geochemistry, Geodynamics. Springer, Heidelberg, 365 pp.

Perini, G., Conticelli, S., Francalanci, L., Davidson J.P., 2000. The relationship between potassic and calc-alkaline post-orogenic magmatism at Vico volcano, central Italy. J. Volcanol. Geotherm. Res. 95, 247–272.

Rosi, M., Santacroce, R., Sheridan, M.F., 1987. Volcanic Hazard. In: Santacroce, R (ed) "Somma-Vesuvius". Quaderni de la ricerca scientifica, CNR, Roma 8, 197-220.

Thibault, Y., Holloway, J.R., 1994. Solubility of CO_2 in a Ca-rich leucitite: effects of pressure, temperature, and oxygen fugacity. Contrib. Mineral. Petrol. 116, 216–224.

Trigila, R., Agosta, E., Currado, C., De Benedetti, A.A., Freda, C., Gaeta, M., Palladino, D.M., and Rosa, C., 1995. Petrology. in: Trigila, R. (Ed.), The Volcano of the Alban Hills. Tipografia S.G.S., Roma, 95– 165.

Turco, E., Zuppetta A., 1998. A kinematic model for the Plio-Quaternary evolution of the Tyrrhenian-Apenninic system: implications for rifting processes and volcanism. J. Volcanol. Geotherm. Res 82, 1-18.

Turi B., and Taylor, H.P., 1976. Oxygen isotopes study of potassic volcanic rocks of the Roman province, central italy. Contrib. Min. Pet. 55, 1-31.

Voltaggio, M., Barbieri, M., 1995. Geochronology. In: Trigila, R. (Ed.), The volcano of the Alban Hills. Tipografia S.G.S., Rome, 167–192.

Figure Captions:

Figure 1

Total Alkali versus Silica diagram of the volcanic products emitted at the Roman Province (after Peccerillo, 2005). For clarity, compositions emitted at Mts. Sabatini are not shown, they would plot between the fields of Vico and Alban Hills.

Figure 2

TAS diagram showing the experimental residual liquids obtained in this study (a), bulk rock and melt inclusion analyses of the Alban Hills eruptive products of the post (b) and pre-caldera (c) periods (after Fornaseri et al., 1963; Trigila et al., 1995; Freda et al., 1997; Palladino et al., 2001; Marra et al., 2003; Gaeta et al., 2006; Giordano et al., 2006). The starting composition AH7a used in the experiments is indicated by a filled square (a, c). Calcite and dolomite doped experiments are distinguished by different colors (black and gray, respectively). Experimental glass compositions are regrouped as a function of the total amount of carbonate added in the experimental charges. The outlined fields are specific to the starting composition of the experiments and are also shown in (b) and (c). In (b) and (c) the small symbols represent the whole rock compositions, while the big, empty symbols represent the glass inclusion data. All data were normalized to 100% on an anhydrous basis.

Figure 3

MgO versus CaO/Al_2O_3 plot showing experimental residual liquids obtained in this study (a), bulk rock and melt inclusion analyses of the Alban Hills eruptive products of the post (b) and pre-caldera (c) periods (after Fornaseri et al., 1963; Trigila et al., 1995; Freda et al., 1997; Palladino et al., 2001; Marra et al., 2003; Gaeta et al., 2006; Giordano et al., 2006). The starting composition AH7a used in the experiments is indicated by a filled square (a, c). Calcite and dolomite doped experiments are distinguished by different colors (black and gray, respectively). Experimental glass compositions are regrouped as a function of the amount of calcite added in the experimental charges. The outlined fields are specific to the starting composition of the experiments and are also shown in (b) and (c). In (b) and (c) the symbols are as in Figure 2, the small symbols represent the whole rock compositions, while the big, empty symbols represent the glass inclusion data. All data were normalized to 100% on an anhydrous basis.

Figure 4

Experimental (black and gray filled circles) and natural (crosses) clinopyroxene compositions. Mg# = MgO/(MgO+FeO). Fe content is calculated as ferrous iron after Lindsley (1983) and CaO amount is normalized to 100%. The same procedure of calculation was followed for both natural and experimental pyroxene compositions. Traced fields group together the experimental clinopyroxene compositions resulting from similar additions of carbonate and are specific to the starting composition of the experiments. Natural cpx compositions are from Aurisicchio et al. (1988); Federico and Peccerillo (2002); Dallai et al. (2004); Gaeta et al. (2006). Three analyses of cpx from low SiO_2, high alkali bulk rock compositions (Aurisicchio et al., 1988) are indicated by an ellipse, while two analyses from high SiO_2, low alkali bulk rock compositions (Aurisicchio et al., 1988) are marked by a square.

Figure 5

Calculated CO_2 emission rates as a function of the magma feeding rate for magmas containing 2500 ppm of CO_2 (solubility at 200 MPa, ref) or assimilating 3, 12 and 15 wt% of carbonates. CO_2 emissions at the Alban Hills are also shown (Chiodini and Frondini, 2001): the intersection of this line with the calculated trends gives the magma feeding rate necessary to provide the measured CO_2 fluxes. The magma feeding rates determined by Chiarabba et al. (1997) and Feuillet et al. (2004), by geophysical modeling (see text) are represented, showing a good agreement with the calculated magma feeding rate for 3-15 wt% assimilation.

Table 1: Experimental conditions, glass compositions and phase proportion.

Temp/sample	Starting glass	1150/1	1150/2	1150/3	1150/4	1150/5	1150/6*
Added calcite wt%	-	-	3.6	-	7	10	10
Added dolomite wt%	-	-	-	6	-	-	-
Glass composition							
SiO_2	48.05	48.18	47.30	46.23	46.06	44.99	44.83
TiO_2	0.96	0.87	0.84	0.86	0.90	0.89	0.81
Al_2O_3	14.60	14.50	14.19	14.45	14.34	15.00	13.63
MgO	6.45	6.50	6.54	7.24	6.34	5.85	6.12
FeO	7.85	7.20	7.13	7.10	7.52	7.07	7.43
CaO	11.40	11.35	12.70	12.65	13.62	15.12	15.63
Na_2O	1.63	1.64	1.63	1.85	1.72	1.86	1.47
K_2O	7.30	7.40	7.45	7.46	7.31	7.07	7.09
P_2O_5	0.51	0.65	0.63	0.67	0.69	0.73	0.60
H_2O	1.25**	1.7**	1.30	1.20	1.21	1.13	2.10
wt % phases							
Glass		100	97.9	94.5	94.2	87.2	94.8
Cpx		traces	0.4	1.6	2.8	6.7	-
Leucite		-	-	traces	0	1.4	-
Olivine		-	-	0.8	-	0	-
Oxides		-	-	-	-	-	-
Fluid		-	1.7	3.06	3	4.6	5.2

* Extra water was added (1.5 wt%)
** Karl Fischer Titration data (+/- 0.25 wt%)

Temp/sample	1100/1	1100/2	1100/3	1100/4	1100/5*	1100/6
Added calcite wt%	-	2.7	5.2	-	5.2	9
Added dolomite wt%	-	-	-	4.9	-	-
Glass composition						
SiO_2	49.25	46.98	44.96	45.92	46.24	44.62
TiO_2	0.92	0.92	1.03	0.75	0.81	0.86
Al_2O_3	17.68	17.03	16.88	18.11	15.70	16.49
MgO	3.91	3.70	3.41	4.36	4.70	3.04
FeO	6.24	6.93	7.25	6.98	6.97	7.40
CaO	7.33	9.53	10.69	8.13	10.89	13.18
Na_2O	2.78	2.34	3.69	3.56	1.99	2.95
K_2O	9.00	9.70	9.05	9.13	8.85	8.93
P_2O_5	0.92	0.90	1.00	1.10	0.70	0.82
H_2O	1.97	1.67	1.75	1.78	2.96	1.39
wt % phases						
Glass	64	59.4	42.3	38.5	77.9	48.7
Cpx	25.60	30.5	38	38.5	17.2	34.2
Leucite	7.90	7.7	16.1	17.4	0	11.8
Olivine	-	-	-	1	-	-
Oxides	2.50	1.1	1.1	1.9	0.7	0.9
Fluid	-	1.3	2.6	2.8	4.2	4.4

All experiments were performed at 200 MPa +/-10. All compositions are normalized to 100%. Water was determined using the "by difference method" on the microprobe analyses (+/-0.6 wt%), or by KFT when specified. Phase proportions were determined using mass balance calculations. Cpx: clinopyroxene; Leuc.: Leucite; Ol.: Olivine; Ox.: Oxides.

Table 1: Continued.

Temp/sample	1075/1	1075/2	1075/3	1075/4	1075/5	1075/6*
Added calcite wt%	-	5	9.3	15	-	6.2
Added dolomite wt%	-	-	-	-	12	4.8
Glass composition						
SiO_2	50.22	47.56	43.98	40.60	44.58	44.58
TiO_2	0.76	0.84	0.87	0.95	0.85	0.85
Al_2O_3	18.53	18.82	16.86	14.98	15.22	18.31
MgO	2.44	2.20	2.69	2.62	3.81	3.39
FeO	4.56	4.87	6.24	6.18	5.98	5.42
CaO	5.12	9.00	11.85	17.26	15.22	9.72
Na_2O	3.80	4.00	4.78	4.52	4.35	2.63
K_2O	9.75	9.19	9.76	9.51	7.61	11.69
P_2O_5	1.17	1.32	1.01	1.72	0.48	0.70
H_2O	3.66	2.20	1.77	1.46	1.58	2.41
wt % phases						
Glass	39.4	30.7	30.1	33.9	33.2	43.5
Cpx	39.3	43.2	45.3	43.2	34.9	42
Leucite	16.6	20.1	17.9	14.4	17.8	6.6
Olivine	-	-	-	-	3.2	trace
Oxides	4	3	1.8	1.2	3	0.8
Fluid	0	2.9	4.8	6.85	6.89	6.92
Contain also	*Phlog.*	-	*Mel.*	*Mel., ap., phlog.*	*Ap., phlog*	-

Phlog.: Phlogopite; Mel.: Melilite; Ap.: Apatite

Temp/sample	1125/1	1125/2	1125/3*
Added calcite wt%	14.5	-	8.2
Added dolomite wt%	-	14	10
Glass composition			
SiO_2	38.98	41.40	42.02
TiO_2	0.95	1.04	0.82
Al_2O_3	15.80	16.92	15.26
MgO	4.21	5.69	6.71
FeO	8.43	7.25	6.15
CaO	17.91	11.90	14.86
Na_2O	3.04	3.91	1.95
K_2O	7.90	9.01	9.41
P_2O_5	1.07	1.27	0.79
H_2O	1.38	1.30	1.73
wt % phases			
Glass	46.2	53.2	63.9
Cpx	34	29	24
Leucite	13	7.75	0
Olivine	-	-	-
Oxides	0	0.5	1.8
Fluid	6.8	7.04	9.28
Contain also			*Phlog.*

Table 2 : Selected analyses of natural and experimental cpx and olivine.

Phase	Cpx	Cpx	Cpx	Cpx	Cpx	Cpx	Ol	Ol
Experimental crystals								
Temp./sample	1150/1	1150/4	1100/1	1100/4	1075/1	1075/3	1150/3	1100/4
SiO_2	53.04	51.69	47.30	45.60	47.09	45.07	41.47	40.97
TiO_2	0.43	0.41	0.96	1.08	0.91	1.17	-	-
Al_2O_3	2.01	3.05	6.26	7.22	8.10	9.73	0.05	0.04
Cr_2O_3	0.40	0.38	0.04	0.07	-	-	0.10	-
MgO	17.49	16.44	13.68	12.06	12.15	10.14	51.84	50.21
FeO	2.21	2.33	6.99	8.09	8.30	8.92	5.28	7.60
MnO	-	0.08	0.42	0.14	-	-	0.25	0.29
CaO	24.10	25.15	23.26	24.63	22.89	24.47	0.96	0.83
Na_2O	0.11	0.14	0.32	0.34	0.20	0.15	-	-
K_2O	0.10	0.14	0.51	0.46	0.15	0.10	-	-
P_2O_5	0.10	0.20	0.26	0.30	0.20	0.25	-	-
F	-	0.22	-	-	-	-	-	-
NiO	0.07	0.02	-	-	-	-	0.04	0.07
Total	99.71	99.93	100.12	99.59	99.46	99.31	99.34	99.81
Natural crystals								
Sample name	AH-3/4	Ca20d	AH17	UFU2	AH1da	AH3-1	BD	CA14
Author	Gaeta	Dallai	Dallai	Gaeta	Dallai	Dallai	Federico	Federico
Age Ka	69	366	<70	366	204	<70	<60	<60
SiO_2	53.12	51.50	48.23	46.77	46.23	45.75	41.73	40.85
TiO_2	0.30	0.50	0.96	1.07	1.40	1.34	-	-
Al_2O_3	2.17	2.57	5.59	6.19	8.13	7.99	-	-
Cr_2O_3	-	0.19	0.10	-	0.11	0.05	-	0.02
MgO	17.36	15.91	13.56	12.17	12.03	10.92	53.25	49.22
FeO	2.84	3.76	6.84	9.12	8.31	9.36	3.70	8.15
MnO	0.10	0.08	0.08	0.15	0.10	0.18	0.24	0.96
CaO	23.95	25.05	24.44	24.26	23.31	24.16	1.07	0.80
Na_2O	0.16	0.45	0.18	0.26	0.35	0.26	-	-
K_2O	-	-	0.02	-	0.01	-	-	-
Total	99.38	98.62	99.77	98.81	99.73	99.18	99.13	100.92

Gaeta: Gaeta et al., 2006; Dallai: Dallai et al., 2004; Federico: Federico et al., 1994.

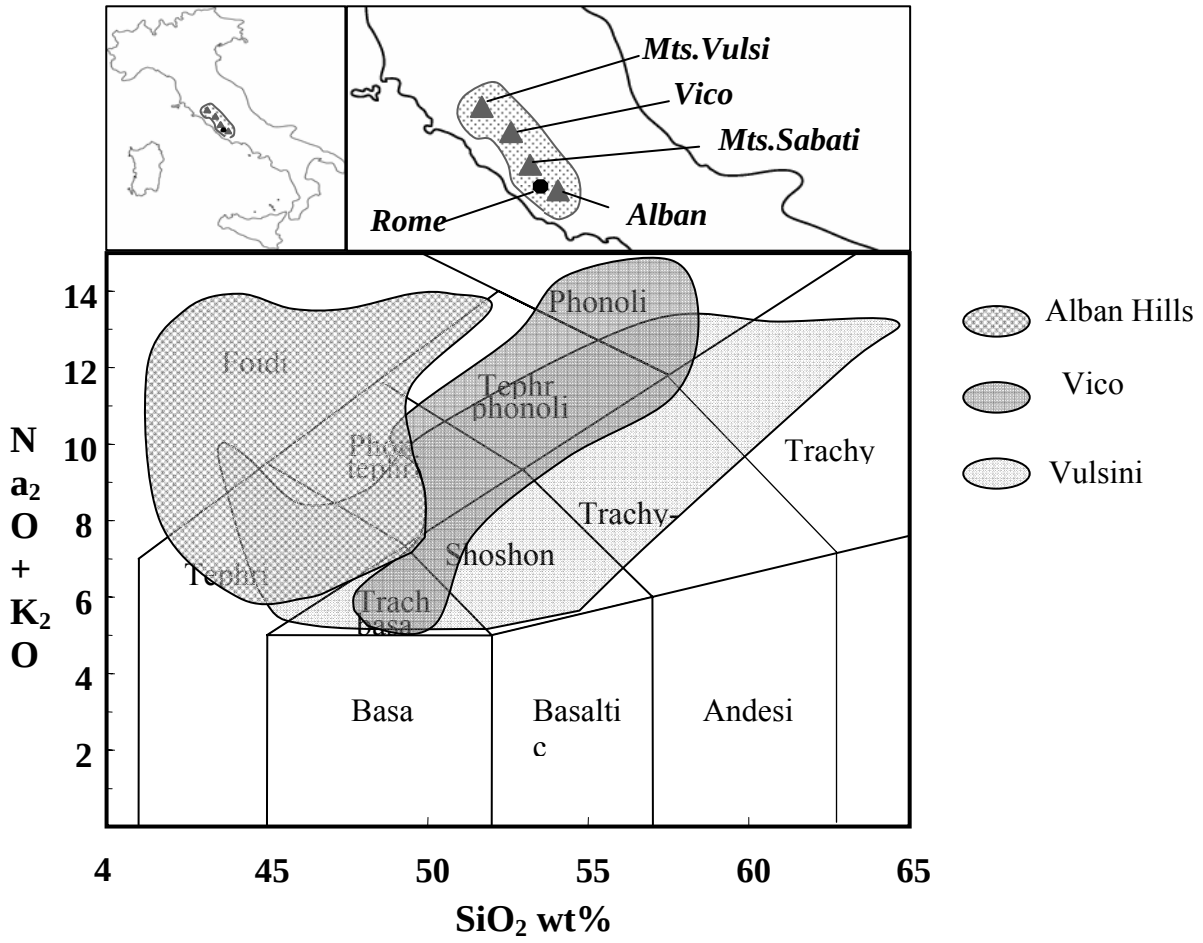
Mts.Vulsi
Vico
Mts.Sabati
Rome
Alban
Phonoli
Foidi
Tephr phonoli
Trachy
Trachy-
Shoshon
Tephri
Trach basa
Basa
Basaltic
Andesi
Alban Hills
Vico
Vulsini
Na2O + K2O
SiO2 wt%
14
12
10
8
6
4
2
4
45
50
55
60
65

Figure 1

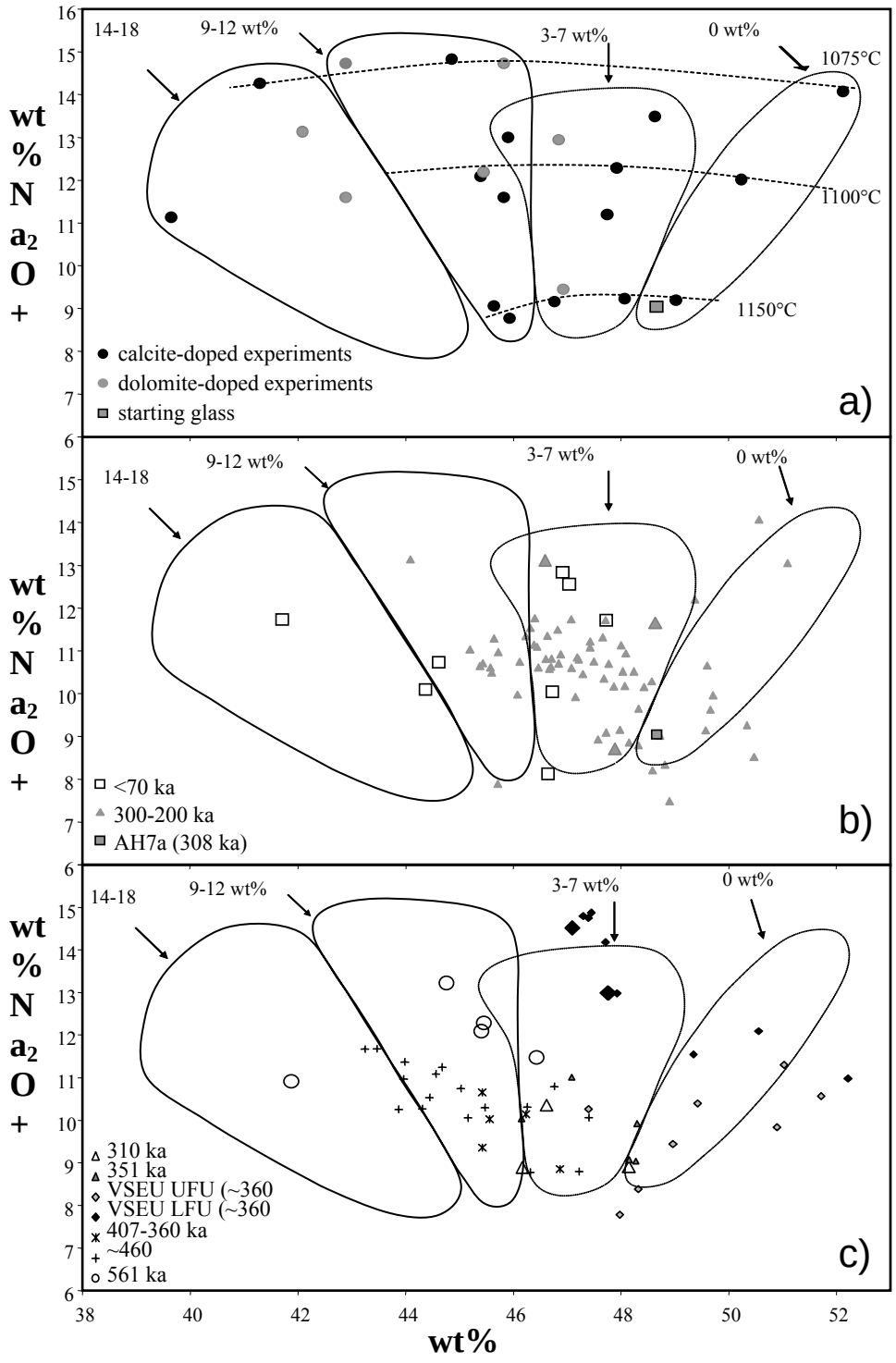
14-18
9-12 wt%
3-7 wt%
0 wt%
1075°C
1100°C
1150°C
calcite-doped experiments
dolomite-doped experiments
starting glass
a)
<70 ka
300-200 ka
AH7a (308 ka)
b)
310 ka
351 ka
VSEU UFU (~360
VSEU LFU (~360
407-360 ka
~460
561 ka
c)
wt% Na2O+
wt%

Figure 2

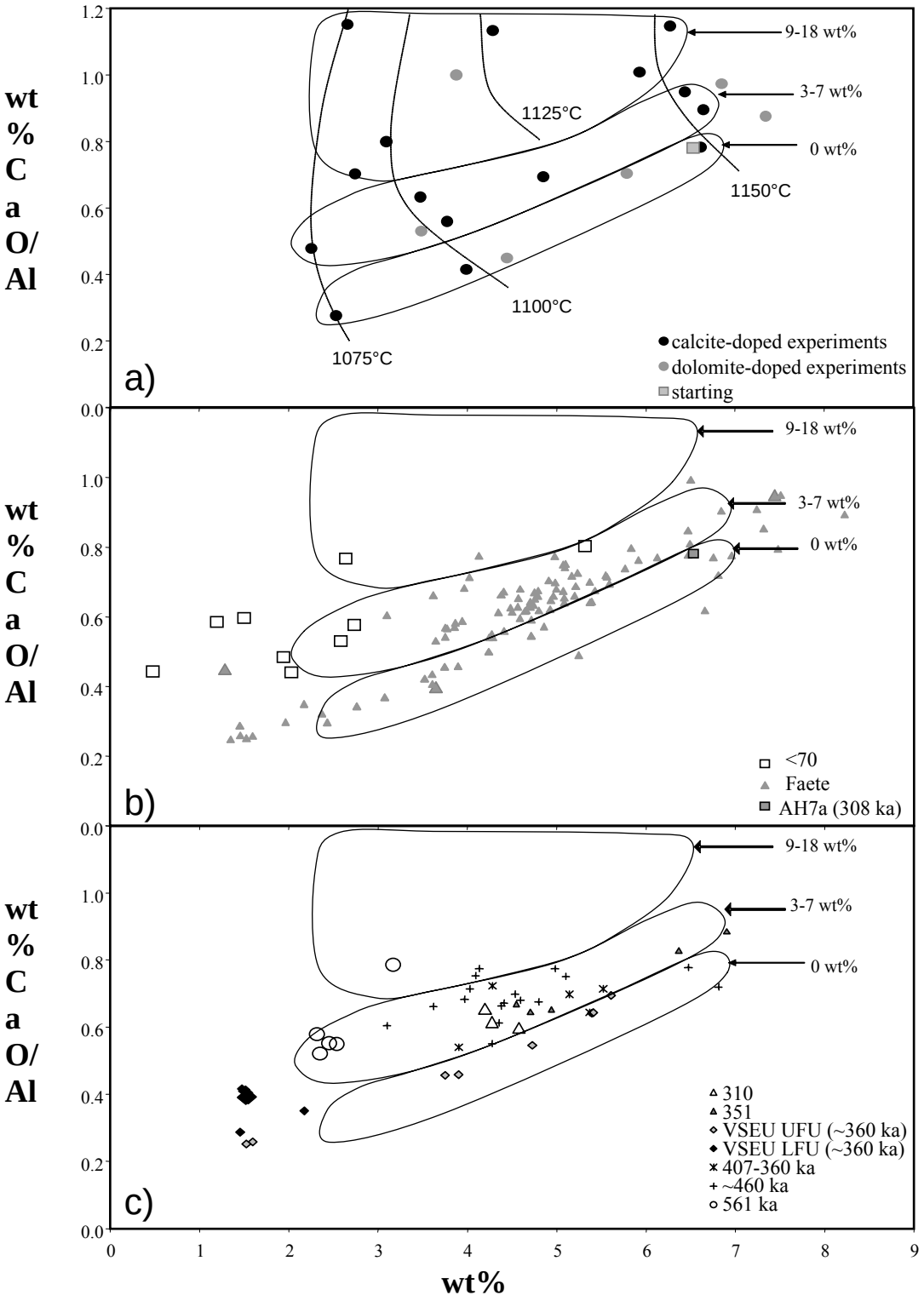
wt % CaO/Al
a)
b)
c)
9-18 wt%
3-7 wt%
0 wt%
1125°C
1150°C
1100°C
1075°C
calcite-doped experiments
dolomite-doped experiments
starting
<70
Faete
AH7a (308 ka)
310
351
VSEU UFU (~360 ka)
VSEU LFU (~360 ka)
407-360 ka
~460 ka
561 ka
wt%

Figure 3

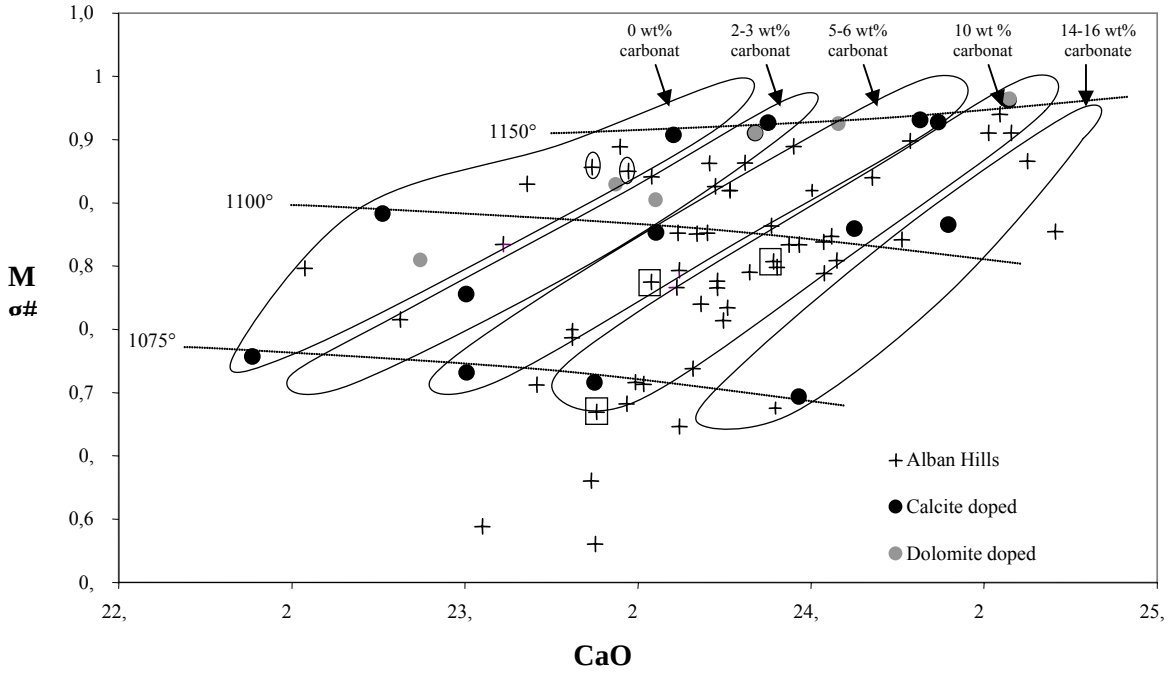
0 wt%
carbonat
2-3 wt%
carbonat
5-6 wt%
carbonat
10 wt %
carbonat
14-16 wt%
carbonate
1150°
1100°
1075°
Alban Hills
Calcite doped
Dolomite doped
M
σ#
CaO
1,0
1
0,9
0,8
0,7
0,6
22,
2
23,
24,
25,

Figure 4

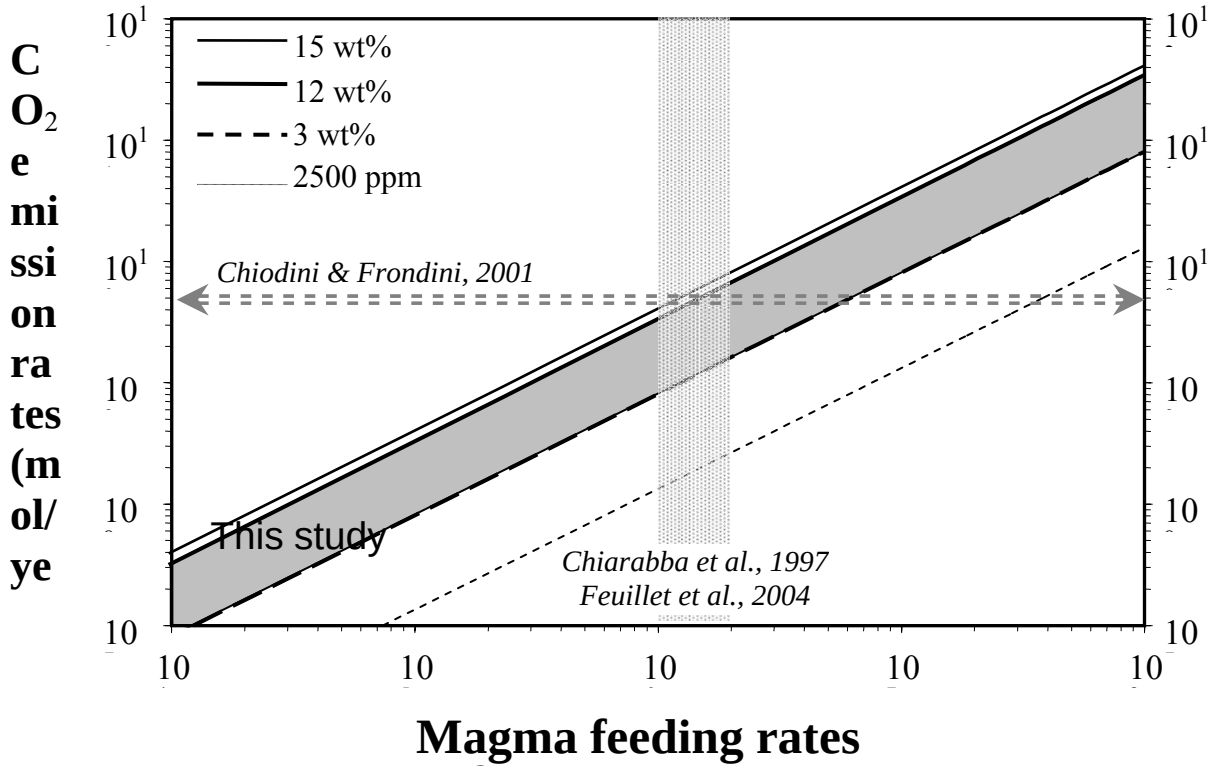
CO2 emission rates (mol/ye
15 wt%
12 wt%
3 wt%
2500 ppm
Chiodini & Frondini, 2001
This study
Chiarabba et al., 1997
Feuillet et al., 2004
Magma feeding rates

Figure 5